Journal of Maps

ISSN: (Print) (Online) Journal homepage: https://www.tandfonline.com/loi/tjom20

The Tachrift channel-levée turbidite complexes (Tortonian) of the Taza-Guercif basin (South Rifian Corridor, NE Morocco)

Fabrizio Felletti , Mattia Marini , Imad El Kati & Hassan Tabyaoui

To cite this article: Fabrizio Felletti , Mattia Marini , Imad El Kati & Hassan Tabyaoui (2020) The Tachrift channel-levée turbidite complexes (Tortonian) of the Taza-Guercif basin (South Rifian Corridor, NE Morocco), Journal of Maps, 16:2, 902-917, DOI: 10.1080/17445647.2020.1844088

To link to this article: https://doi.org/10.1080/17445647.2020.1844088

JOURNAL OF MAPS
2020, VOL. 16, NO. 2, 902–917
https://doi.org/10.1080/17445647.2020.1844088

Taylor & Francis
Taylor & Francis Group

Science

The Tachrift channel-levée turbidite complexes (Tortonian) of the Taza-Guercif basin (South Rifian Corridor, NE Morocco)

Fabrizio Felletti[a], Mattia Marini[a], Imad El Kati[b] and Hassan Tabyaoui[b]

[a]Dipartimento Scienze della Terra 'A. Desio', Università degli Studi di Milano, Milano, Italy; [b]Natural Resources and Environment laboratory, Polydisciplinary Faculty of Taza, Sidi Mohamed Ben Abdellah University, Taza, Morocco

ABSTRACT

This contribution reports on the field mapping of 9 exceptionally well-exposed channel-levée complexes from Taza–Guercif Basin (NE Morocco), belonging to the Late Miocene Tachrift turbidite system. Separated from each another by hemipelagic marlstones, the mapped channel-levée complexes exhibit thicknesses in the range of 5–25 m. Four main sedimentary facies associations were mapped, including channel-fill sandstones, levée thin-bedded heterolithics, chaotic mass transport deposits, and hemipelagic marlstones. In addition, two end-member styles of channel-fills spatial stacking were recognized, reflecting different modes of channel belt development and/or location along the slope profile, namely: (a) a lateral-migration pattern, resulting from lateral migration of high-sinuosity levéed channel belts, as opposed to (b) a vertically stacked pattern, interpreted to reflect the vertical aggradation of levéed channel belts with a relatively low sinuosity. The geological map accompanying this contribution provides the basis for more in-depth sedimentological investigations on the channels of the Tachrift turbidite system.

ARTICLE HISTORY
Received 6 May 2020
Revised 22 October 2020
Accepted 27 October 2020

EYWORDS
Channel; levée; turbidite; Taza-Guercif basin; Tachrift turbidite system; Tortonian

1. Introduction

Submarine channels constitute an important component of both fossil and modern submarine fans, as well as an attractive target for hydrocarbon exploration (Weimer et al., 2000). Despite being the focus of sedimentological research over the last few decades (e.g. 2002; Campion et al., 2003; Cronin, 1995; Cronin et al., 2000; Di Celma et al., 2011; Felletti, 2016; Fonnesu, 2003; 2019; Gardner et al., 2003; Hansen et al., 2015; Hubbard et al., 2014; Kneller et al., 2020; 2003; Sullivan et al., 2000; Sylvester et al., 2011; Walker, 1975; Wynn et al., 2007), well-exposed outcrops of turbidite channels and coeval levées are relatively rare and thus poorly documented, at best by sets of two dimensional exposures. Examples include the classical outcrops of Canyon San Fernando, Mexico (Kane et al., 2007; Li et al., 2018), the Brushy Canyon, West Texas (Pyles et al., 2010), the PabRange, Pakistan (Eschard et al., 2003), the Magallanes basin, southern Chile (Macauley & Hubbard, 2013), and the Karoo basin, South Africa (Figueiredo et al., 2013), which depict a large variety of depositional style resulting from multiple interplaying controls.

Despite recent advancement in seismic acquisition providing unprecedentedly detailed 3D images of subsurface examples (e.g. Janocko et al., 2013), resolution is still too low and lithological information from boreholes too sparse to provide insights into sedimentary heterogeneity of channel-levee deposits. As a result, well-exposed extensive outcrops still represent a very valuable source of insights into depositional architecture of channelized turbidites and linked sedimentary processes.

This contribution reports on the field mapping of nine superbly exposed turbidite channel-levee complexes (the Tachrift Turbidite Subunit of Gelati et al., 2000), which represent part of the clastic infill of the Late Miocene Taza–Guercif Basin of NE Morocco (Figure 1). The geological map accompanying this contribution (Annex 1) aims to document location, lateral continuity and arrangement of the component architectural elements (i.e. sand-prone channel-fills, levées, Mass Transport Deposits and intervening hemipelagic deposits) of these channelized turbidite complexes, thereby providing the basis for more in-depth sedimentological investigations.

2. Geological setting

The Taza-Guercif basin (TGB, Figure 1(a)) of northeastern Morocco was part of the Rifian Corridor, a seaway which connected the paleo-Mediterranean with the Atlantic Ocean during the late Miocene. The Rifian Corridor is regarded as the remnant part of the foreland basin developed to the south of the

CONTACT Fabrizio Felletti fabrizio.felletti@unimi.it Dipartimento Scienze della Terra 'A. Desio', Università degli Studi di Milano, via Mangiagalli 34, Milano 20133, Italy

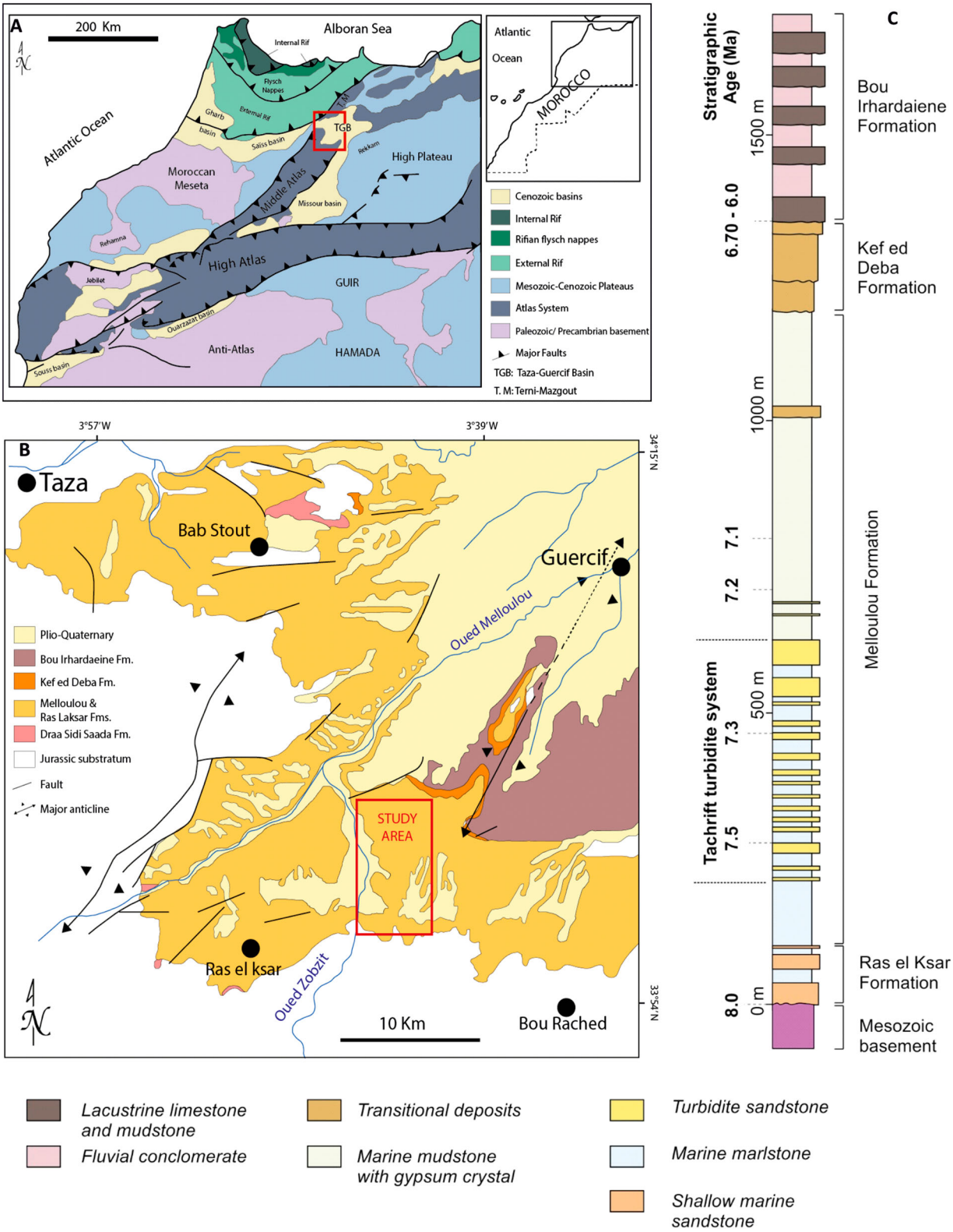

Figure 1. (a) Geological sketch map of northern Morocco depicting the spatial relationship of the Guercif basin to other major Cenozoic tectonic elements of Morocco, including the Rif and Atlas mountains (modified after (Pratt et al., 2016)); (b) geologic map of the Taza-Guercif Basin (modified after Krijgsman et al., 1999). Box denotes the study area. (c) Stratigraphic succession of the sediment fill of the southern Taza-Guercif Basin (modified, Pratt et al., 2016) with age from magnetostratigraphy after (Krijgsman et al., 1999).

external thrust front of the Rif mountains (Bernini et al., 2000) (Figure 1(a)). Belonging to the Betic-Rif orogenic system of western Mediterranean Sea (Figure 1(a)), the Rif mountains represent the product of tectonic accretion at the edge of the Alboran micro-continent during the Cretaceous–Miocene convergence of the African and Eurasian Plates (Chalouan et al., 2008; de Lamotte et al., 2009).

The Taza-Guercif basin (Figure 1(b)) is regarded as a 'post-Nappes' extensional basin formed since the late Tortonian as a result of extensional reactivation of the Middle Atlas rift faults, interpreted to reflect loading (foreland flexure) by the external Rif thrust (Bernini et al., 2000; Sani et al., 2000), or the far-field affect of deformation in the central Rif (2000).

In the Taza-Guercif basin, the Tortonian extension was followed by the deposition of a transgressive-regressive sequence of continental to deep-water marine deposits up to ca. 1500 m-thick, spanning in age from the late Tortonian to the early Pliocene (Bernini et al., 1999) and comprising five main lithostratigraphic units (Figure 1(c)). Presently, this succession is deformed by a series of NE-SW striking tectonic features likely to reflect a transpressive activity (1990; El Kati et al., 2017).

2.1. The study area

The mapped area is represented by the extensive outcrop laying to the east of the Zobzit River (Figure 1(b)) opposite Douar Tachrift where a particularly well-exposed section of the late Tortonian-early Pliocene fill -ofthe Taza-Guercif basin crops out underlying a once widespread suite of Plio-Quaternary continental deposits.

Here, the late Tortonian marine transgression is defined by the onlap of the up to 100 m-thick shallow marine clastic sediments of the Ras El Ksar Formation (Figure 1(c)) on top of the Jurassic basement of the Middle Atlas. Comprised by a variety of lithologies (biolithites, sandstones, siltstones and mudstones) that alternate and interfinger over short scales, the Ras El Ksar Formation is key for the late Miocene paleogeography of Morocco because it marks the opening of the Rifian corridor (Bernini et al., 1999; 1990; Gelati et al., 2000)

As a result of continued tectonic subsidence, The Ras El Ksar Formation gradually transitions upward into the Melloulou Formation (Bernini et al., 1999), a several hundred meters-thick (100–1200 m) sedimentary package dominated by grey to blue hemipelagic marlstones which can be traced through the entire Rifian Corridor.

In the study area, the Melloulou Formation include two turbidite-rich units supplied from the south (from older to younger, the El Rhirane and the Tachrift turbidite sub-units; Bernini et al., 1999; Gelati et al., 2000) with sediments from the Middle Atlas (Pratt et al., 2016), which are juxtaposed in a eastward migrating fashion suggesting a likewise shift of depocentre.

Extensively exposed to the east of the Zobzit River (Figure 1(a)), the Tachrift unit is ca. 600 m thick and comprises 15 main sand-prone bodies, each a few tens of m thick, separated by marsltone packages of similar thickness. Characterized by lenticular geometry and erosive base, the sand-prone bodies show lateral continuity of a few hundred of metres and a transition into laterally persistent packages of thin-bedded turbidites (Gelati et al., 2000).

The Tachrift turbidites rapidly grade upward to the gypsiferous marlstones constituting the upper half of the Melloulou Fm (Figure 1(c)) and dated to the Messinian (Krijgsman et al., 1999; Krijgsman & Langereis, 2000).

The thick gypsiferous marlstone of the upper Melloulou Formation are in turn sharply overlain by the near-shore to intertidal sandstones and calcilutites of the Kef Ed Deba Formation (Figure 1(c)), which indicates a rapid relative sea-level drop (Bernini et al., 1999; Krijgsman et al., 1999). Such a regressive phase culminates in the final emergence of the Taza-Guercif Basin with the formation of the Messinian regional unconformity (6.7-6.0 Ma; Krijgsman et al., 1999; Krijgsman & Langereis, 2000) and would reflect compressional tectonics and regional uplift resulting from encroachment of the south-vergent Rifean thrust front on the Middle Atlas structure (Bernini et al., 1999, 2000).

The Zobzit succession terminates with the Pliocene Bou Irhardaiene Formation (Gelati et al., 2000) represented by more than 400 m of continental conglomerates, calcarenites and lacustrine calcilutites sitting on top of the Messinian unconformity.

3. Methods and materials

The 1:5000-scale geological map (Annex 1) accompanying this contribution covers an area of approximately 16 km^2 surveyed between November 2018 and February 2019. We used a 1:5000 scale high-resolution print of Bing Maps Aerial Imagery as a base map with the overlay of a vector version of the official 1:50,000 scale topographic map of the Kingdom of Morocco. The excellent exposure quality (Figure 2), coupled with easy access to outcrops and walkability allowed us to map 9 turbidite channel-levée bodies (labelled 1–9 in Annex 1) with thickness in the range of 5–25 m.

Following the hierarchy proposed by (Gardner et al., 2003), the elemental building block of the mapped turbidite bodies is represented by single-storey channel belt and associated levées (Figure 2 (b)), which record the life cycle of a turbidite channel from cutting of its basal erosion to its fill and spill and consequent build-up of coeval levées. As single-storey channel belts are comprised of multiple subsequent events of erosion and sediment filling, their overall shape and internal architecture can show considerable variability as a result of contrasting migration pathways of the channel (vertical aggradation vs. lateral migration; Figure 2(b,c)). Single-storey channel-fills and levées can stack spatially with a common

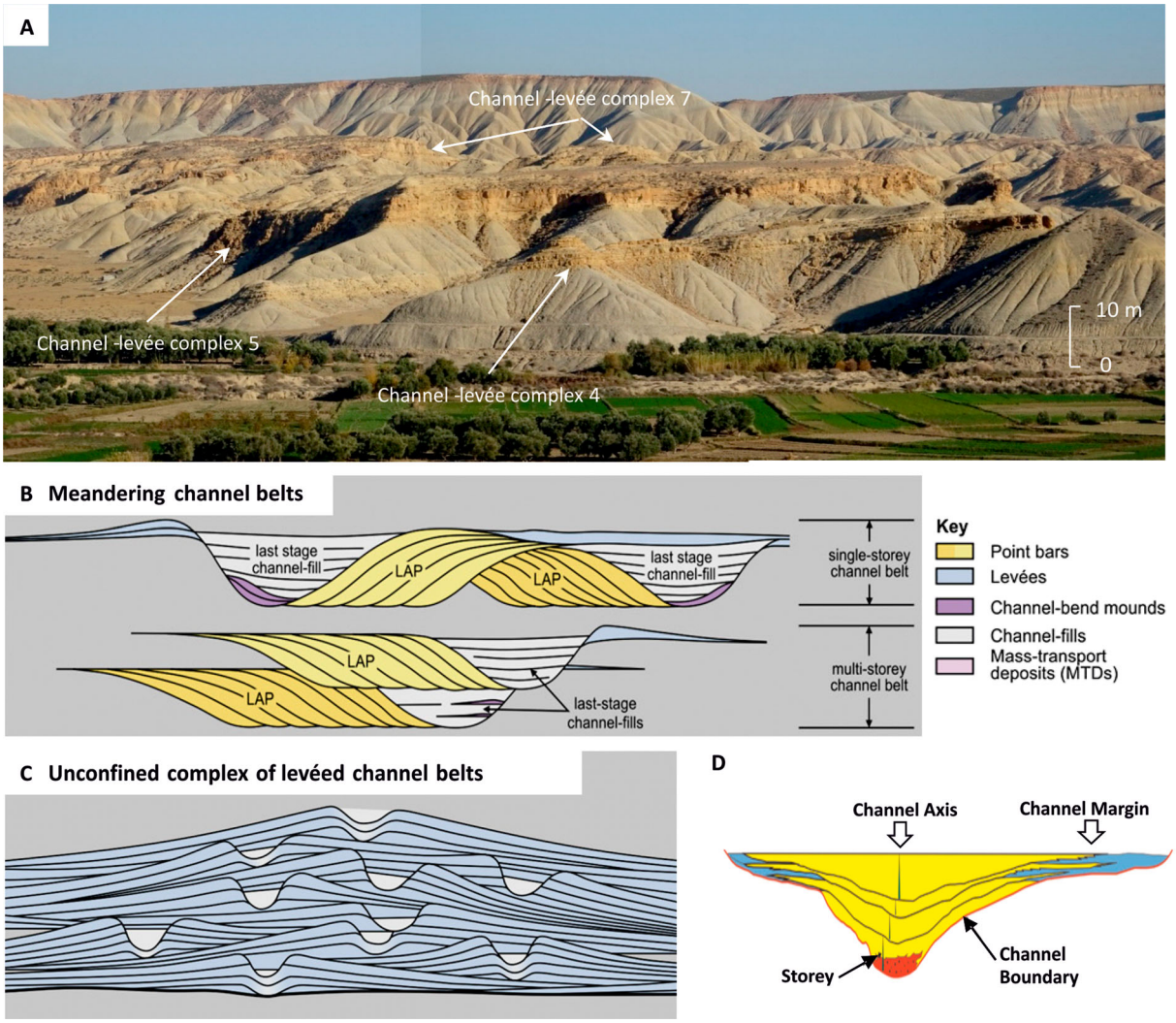

Figure 2. (a) panoramic view of part of the study area to the east of the Zobzit River, opposite Douar Tachrift; (b) and (c) hierarchy of turbidite channel-levee deposits systems adapted from Janocko et al. (2013). Note that aspect ratio, internal architecture and spatial staking of single storeys and higher rank units are highly idealized; (d) Internal architectural variability within an aggradational channel-fill. Note that the sand-prone channel axis fill may include lateral accretion packages.

migration pathway so to form a multi-storey channel belt (Figure 2(b)). Finally, a few to several subsequent channel belts and associated levées stack spatially (locally eroding into older ones) to form each of the nine channel-levée complexes (Figure 2(c)) mapped in Annex 1.

Based on dominant lithology and primary sedimentary characteristics, we distinguished and mapped out four main facies assemblages (section 4), each reflecting a specific depositional element of a turbidite slope channel.

To locate (with precision less than ca. 5 m) main lithological contacts (e.g. base and top of the mapped complexes), point features (e.g. channel-forms and outcrops of methane derived authigenic carbonates) and bed attitude and palaeocurrent measurements (e.g. orientation of channel-form axes and sole marks and dip-direction of cross- lamination/stratification) we used a Garmin a GPSMAP60CSx global positioning system.

4. Mapped facies associations

4.1. SAND-PRONE CHANNEL-FILLS

Degree of bed amalgamation and sandstone to mudstone thickness ratio gradually decrease moving away from axial and thicker part of a channel form (Figure 3(a,b)) making possible to distinguish and map (Annex 1) two contrasting facies associations typical of channel axis (Section 4.1.1) and channel margin locations (Section 4.1.2). Widths and thicknesses of single-storey channel-fills typically fall in the ranges of 10–50 m and 2–5 m, respectively. However, there are a few more laterally continuous examples reaching a lateral continuity of up to several hundred metres (e.g. Figure 3(c)), which reflect accretion at the bends of laterally migrating sinuous channels (see Section 4.1.1). At higher hierarchical levels (i.e. multi-storey and channel-complex), the lateral continuity of channel-fill geobodies is highly variable.

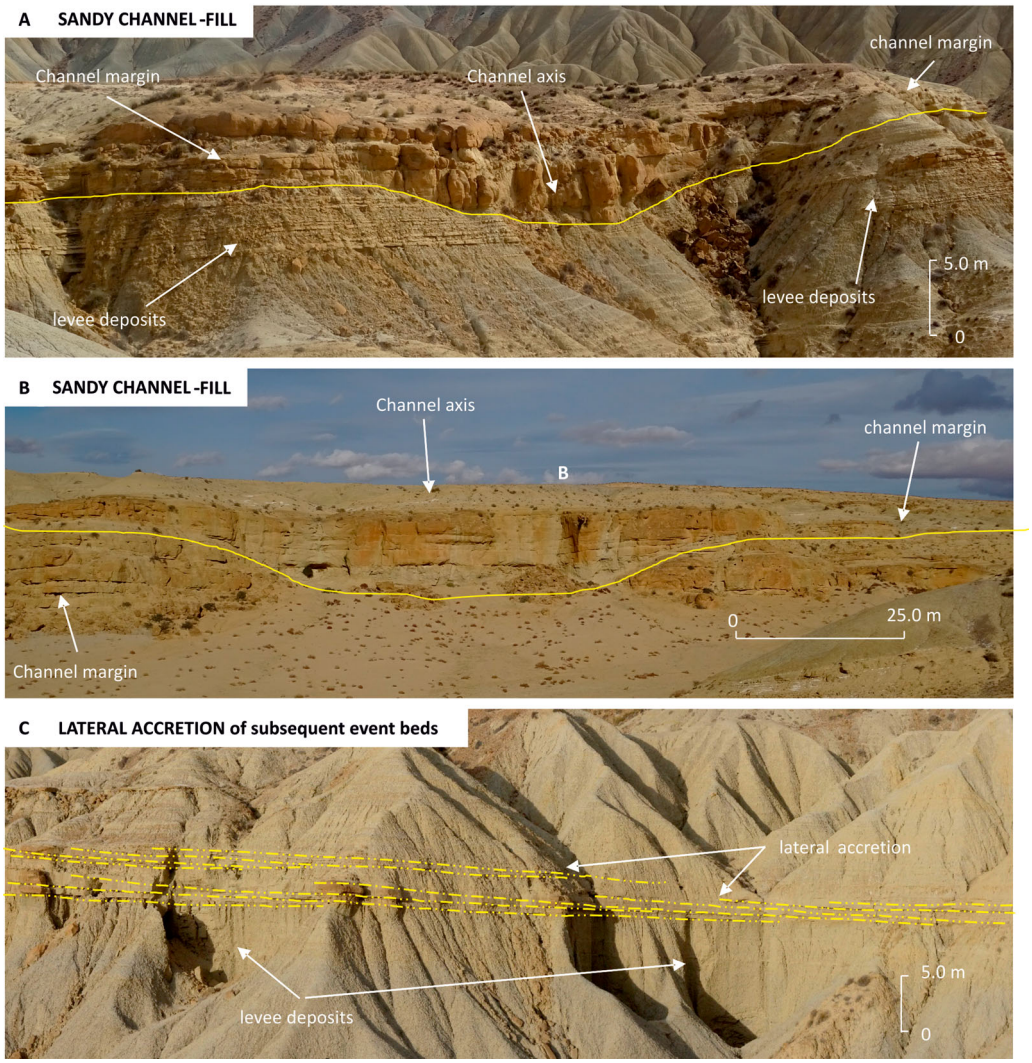

Figure 3 – Strike-section view of the Channel-levée complex 8 (a) and of the Channel-levée complex 7 (b) showing the variety of stratal pattern and degree of bed amalgamation moving away from channel-form axis (palaeoflow is away from viewer); (c) strike-section view of the Channel-levée complex 4. Note the high continuity of amalgamated bedsets resulting from lateral accretion of subsequent event beds.

4.1.1 Channel-Axis – amalgamated coarse-grained turbidite sandstones

These are represented by bed sets of amalgamated sandstone with thicknesses in the range 0.3–2.0 m which become progressively less amalgamated moving off the channel-axis and up-section (Figure 4). Component beds are medium to thick-bedded and have sharp erosive bases, which can locally down-cut into the underlying strata as deep as c. 1.0 m. Sole marks are very rare but a few flute casts indicate paleoflow towards the N.

Channel-axis sandstones are by definition contained within composite erosional surface sculpted during the life cycle of the channel from inception to final fill. The axis orientation of 115 channel forms indicates a dominant class in the range 345°–40°, although a few measurements indicate a more WNW-ESE orientation (see rose diagram in Annex 1).

On outcrop faces perpendicular to palaeoflow, the internal stratification of some amalgamated channel-fills gently dips (2°-6°) suggesting lateral accretion of subsequent beds with sigmoidal shape (Figure 4(a-d)).

Individual sandstones beds commonly show normal grading, with a seemingly structureless coarse-grained basal division (Figure 4(e)) which is generally poorly sorted and can be initiated with a lag of outsized clasts (granule to pebble; Figure 4(f)) or mud rip-ups organised into traction carpets. This basal facies may grade upward into parallel-laminated medium- to fine-grained sandstone (Figure 4(g)) which may be partly cut by subsequent erosion. Erosion and quick infill of basal scours by subsequent flows can result in low to high-angle 'cut and fill' cross laminations.

Conglomerates (Figure 5(a–c)), typically with a poorly sorted sandy-muddy matrix, which become more abundant upward, are rare but present especially close to base of channel-fills where they form thin to medium lenticular beds with a lateral continuity of up to a few tens of metres. Clasts are well rounded

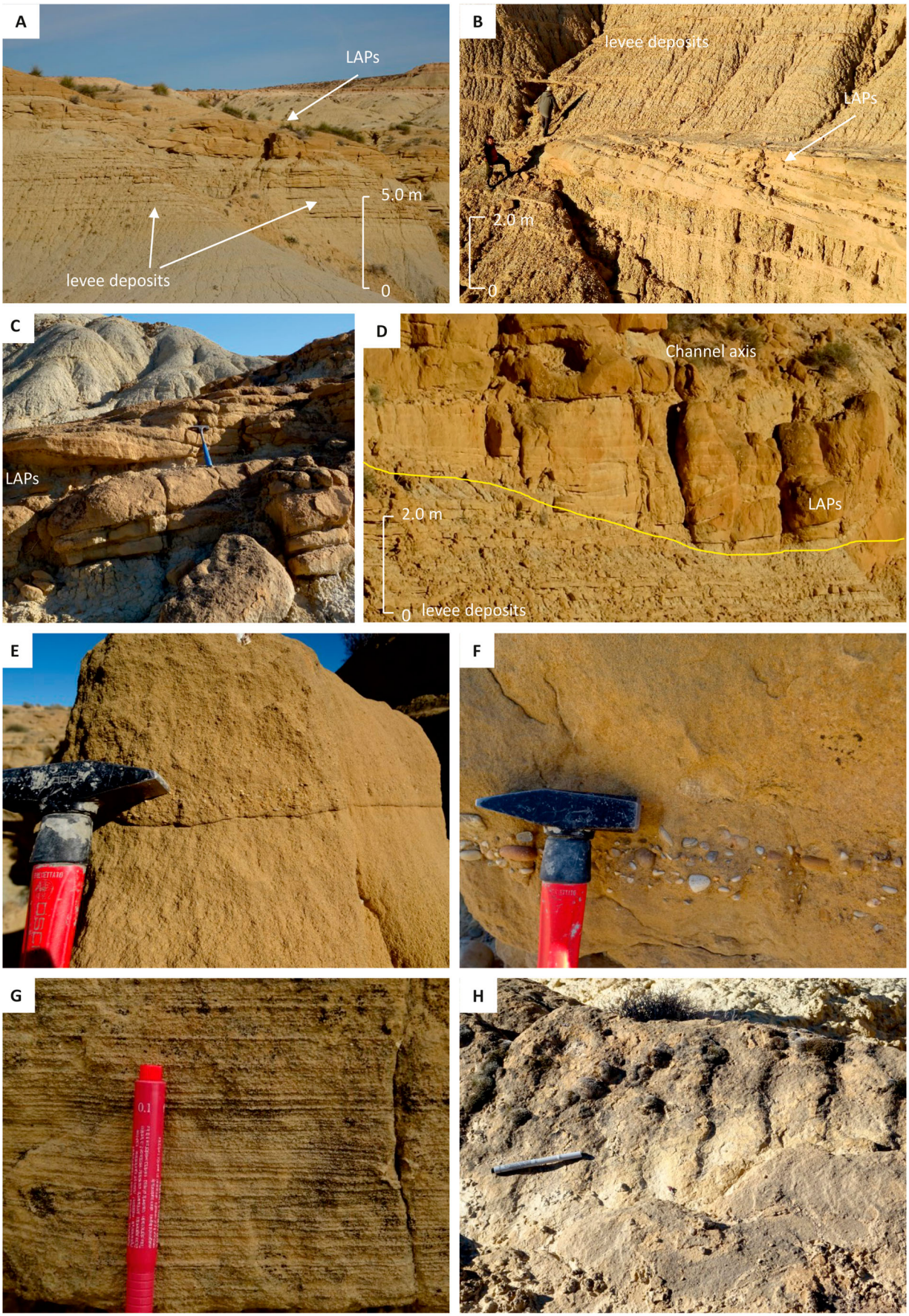

Figure 4 – Laterally accreted sandstone beds from channel-levee Complex 8 (a, d), Complex 4 (b) and Complex 3 (c), interpretable as Lateral Accretion Packages (LAPs) formed at bends of sinuous turbidite channel. Channel-axis normally graded sandstones with (e) traction carpets and crude planar-parallel lamination; (f) pebbly sandstone. Note the coarse-tail inverse then normal grading; (g) planar-parallel laminations; (h) ripple crests.

and poorly to well-sorted with size in the range of fine to medium pebbles (Figure 5(a)). Large sub-rounded mudstone and marlstone rip-up clasts (up to 25 cm in diameter) can be present and abundant in this facies, whereas trace fossils are typically absent (Figure 5(b,c)).

Up-section and/or laterally, basal scouring and bed amalgamation can become progressively less severe resulting in a higher preservation potential of fine-grained cross-laminated bed tops (Figure 4(h)) and intercalations of thin-bedded turbidites and bioturbated mudstones (with traces of *Scolicia* – Figure 5 (d,e,f) – and *Ophiomorpha,* Figure 5(g)) more typical of channel margin settings (see sections 4.1.2). Alternatively, amalgamated channel-axis sandstones can be sharply overlain by intensely bioturbated siliciclastic mudstones (Figure 5(h)) with rare very thin sandstone beds and *Rhizocorallium* traces fossils.

Interpretation: basal scouring and channelling into previous deposits suggest energetic, possibly waxing, parent flows capable of relatively deep erosion at least in an early channel-inception phase. Sedimentary structures indicate traction of bed-load material (with outsized clasts) and high-rate of sediment fall-out from suspension, which altogether suggest deposition in an upper-flow regime from high-density flows. Laterally accreted beds (Figure 4(a–d)) represent Lateral Accretion Packages (LAPs) and are suggestive of deposition within sinuous to meandering channel. Up-section, the transition to better stratified, less amalgamated facies typical of channel margin settings (sections 4.1.2) can reflect progressive lateral shift of the channel-axis. On the other hand, capping of channel-axis sandstones by bioturbated mudstones can be interpreted to record channel abandonment due to up-dip avulsion (Cronin et al., 2000; Hubbard et al., 2014; Kane et al., 2007; McHargue et al., 2011).

4.1.2 Channel Margin – Non-amalgamated medium to thin-bedded sandstones

This facies association dominantly consists of beds sets of medium to thick-bedded sandstone-mudstone couplets (Figure 3), locally interbedded with very thin-bedded heterolithic packages more typical of levées (see section 4.2). The lower part of sandstone beds is generally medium-grained, can show crude laminations associated with dish and pillar dewatering structures but is more frequently planar parallel-laminated, and grades upward into rippled finer-grained silty sandstones. Mudstone caps are silt-rich and rarely thicker than a few centimeters, with sharp contact with the underlying co-genetic sandstone. The geometry of event beds is tabular (Figure 6(a,b)) over most of their length, with rapid lateral tapering at the channel bank.

Both the sandstone and mudstone components of this facies association show very sparse to intense bioturbation with *Scolicia* and *Ophiomorpha* trace fossils (Figure 5(d–g)), albeit the former is by far the most typically ichnotaxon.

Interpretation: sedimentary structures characterizing this facies association suggest deposition from a range of high to low-density turbidity currents with limited erosive ability. The overall tabular geometry of event beds and their quick tapering at channel margins would indicate deposition away from the channel axis, within channels with levéed margins sufficiently super-elevated to partly contain the flow. The multiple thickening-thinning motifs, including the intercalation of packages of very thin bedded heterolithics, may be interpreted to reflect repeated lateral shifts of the channel axis (Cronin et al., 2000; Hubbard et al., 2014; Kane & Hodgson, 2011).

4.2. Heterolithic levée deposits

This facies association comprises very thin-bedded sandstone-mudstone couplets intercalated with a few to several cm-thick beds of hemipelagic marlstones and form laterally continuous sedimentary packages that can partly interfinger with channel-fills (Section 4.1) and show a lateral continuity of several hundreds of metres (Figure 3 and Figure 6(c,d)). These heterolithic deposits are easily distinguishable both in the field and on satellite imagery thanks to their more yellowish hue compared to the background hemipelagites (Section 4.4). Component beds are a few cm-thick $T_{c\text{-}e}$, and $T_{d\text{-}e}$ incomplete Bouma's (1962) with basal grain size rarely coarser than fine sand grade. Starved ripples forming discontinuous trains with lengths of a few metres. Importantly, sandstone proportion decrease uniformly away from channel margins (as documented from numerous modern levée deposits; Piper et al., 1999), which makes correlatability of beds across outcrops practical only in the close reach of sand-prone channel fills.

Deposits are intensely bioturbated, with the most common trace fossil assemblages containing *Scolicia* and *Ophiomorpha* (Figure 5(d–g)) in sandstones, and *Planolites* and *Rhizocorallium* in mudstones (Figure 5(h)).

Interpretation: this facies association is the product of repeated overbank deposition from the less concentrated (and finer-grained) upper part of the suspension cloud of the turbidity currents transiting within channels. The observed change in sandstone content across the mapped levee keeps with the notion that, because of flow expansion, over-spilling flows might have quickly lost capacity to carry sand away from the levee crest. As a result, proximal levées are expected to be associated with a relatively more accentuated topography and lateral change in sand content compared to the muddier and flatter distal levee.

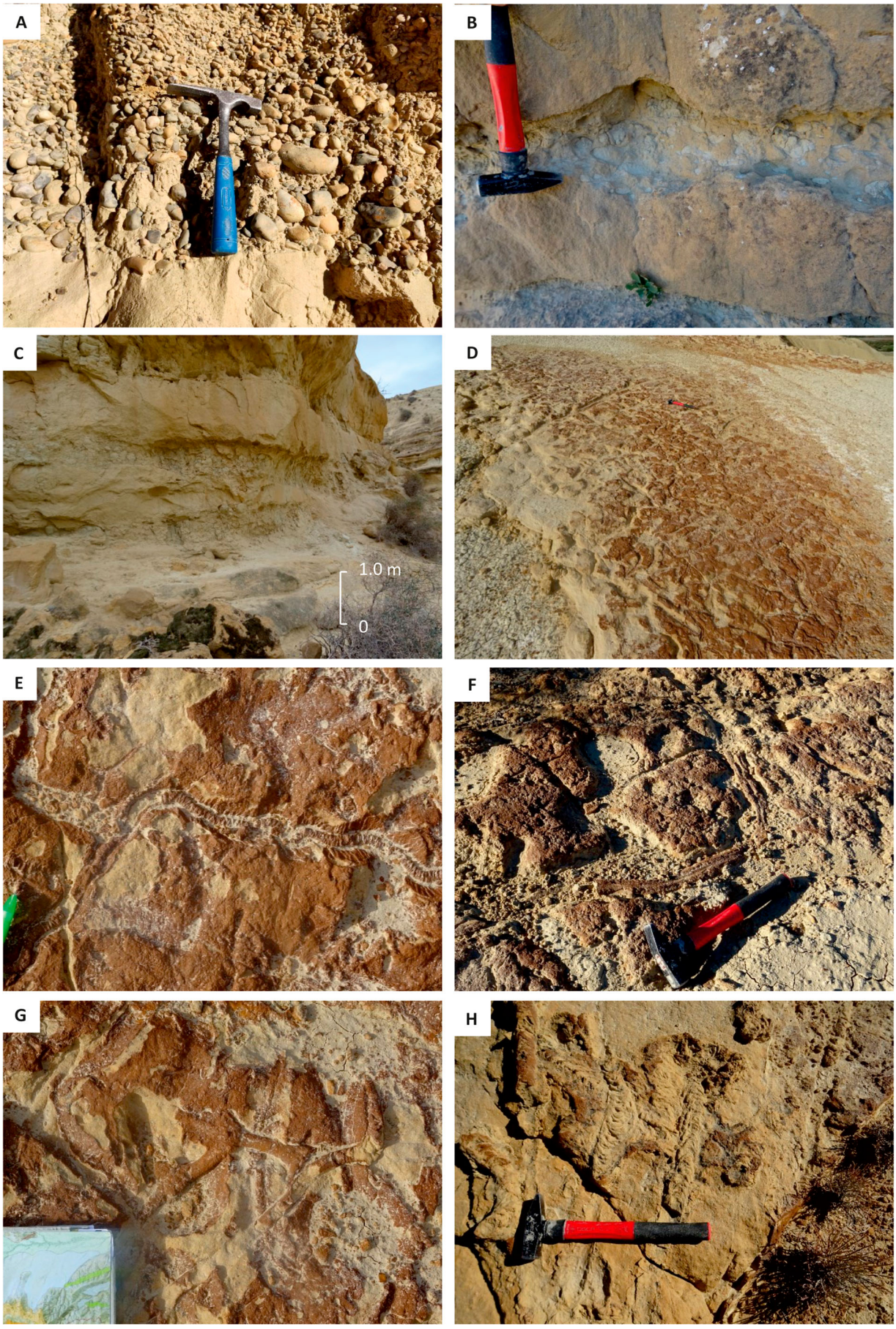

Figure 5. (a) Conglomeratic beds characterized by a variety of clasts, including well-rounded extraclasts of Mesozoic carbonate rocks from the Middle Atlas, poorly to well-sorted and normally graded, and (b), (c) mudstone clasts with variable roundness floating in a mud-rich matrix. Examples of ichnofabrics observed in the sand-prone channel-fills containing *Scolicia* (d) (e) and (f), *Ophiomorpha* (g) and *Rhizocorallium* (h)

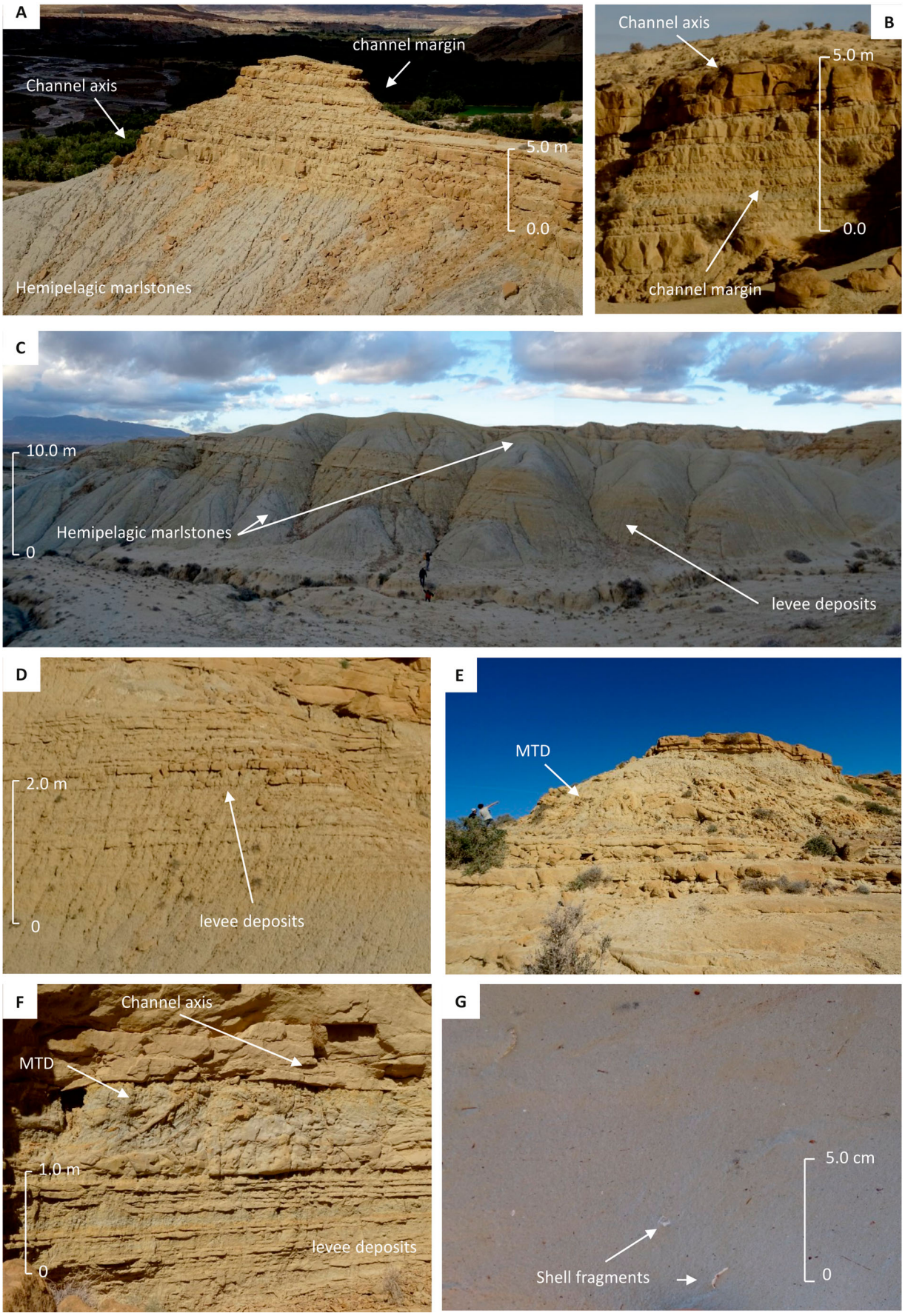

Figure 6. (a) Overview of a channel belt margin belonging to the Channel-levée complex 4. Palaeoflow was perpendicular to the outcrop. (b) Close-up of the channel and laterally equivalent fine-grained channel margins belonging to the Channel-levée complex 6. Fine-grained heterolithic levée deposits of Channel-levée complexes 4 (c) and 8 (d). Mass Transport Deposits (MTDs) characterized by distorted and overturned beds and displaying small scale extensional and compressional structures, belonging to the Channel-levée complex 8 (e) and 5 (f). Hemipelagic marlstones (g) showing small fragments of thin molluscan shells

4.3. Mass transport deposits (MTDs)

These deposits (Figure 6(e,f)) represent a volumetrically small but sedimentologically significant component of the Tachrift channel complexes. Due to their nature, MTDs have irregular tops and highly variable thickness (maximum observed thickness is 5 m). They typically occur in the lower part of the thicker channel-fills (e.g. Complex 7 and 2) where they generate an uneven topography healed by the deposit of subsequent turbidity currents. The internal character of these deposits varies from mildly deformed slide-blocks with intact stratigraphy to chaotic bodies with intensely deformed and/or overturned stratigraphy, locally cut by shear zones where strain resulted in full homogenization of the deposits.

Interpretation: these deposits represent the product of mass wasting of sedimentary packages becoming unstable because of focused erosion of previously deposited channel-margin and levée deposits. Similar deposits are documented from a number of modern and ancient examples of turbidite channels where they can modify the channel morphology at a range of scales and thus significantly condition the sedimentary architecture (Armitage et al., 2009; Mayall et al., 2006; Mayall & Stewart, 2012; Posamentier & Kolla, 2003).

4.4. Hemipelagic marlstones

These deposits are represented by a few metres to a few tens of metres-thick monotonous packages of marlstones with massive appearance and a grey to blue hue (Figure 6(a,c)), intercalated by rare mm-thick very-fine sandstone and siltstone beds are interpreted to represent the distal product of turbidite levees (section 4.2). The marlstone contains both benthic and planktonic foraminifera and occasionally small fragments of molluscan shells (Figure 6(g)). Bioturbation is relatively infrequent, especially compared to what observed in levée deposits and atop sand-prone channel-fills. Most of the sedimentary packages comprised of these marlstones are laterally continuous across the whole study area, thereby separating subsequent turbidite complexes.

Interpretation: these marlstones are interpreted to be dominated by continued hemiplegic fall-out coeval to deposition of the Tachrift channel-levée complexes.

4.5. Methane derived authigenic carbonates

These are represented by carbonate concretions and micrite beds (Figure 7) with the former showing variable shape, ranging from oblate to prolate, and rugose outer surface. Disregarding their shape, concretions occur in the hemipelagic marlstones (section 4.4) and relatively more rarely in levée deposits (section 4.2), and all share a common internal structure. This is comprised of a series of subsequent envelops of authigenic carbonates, with locally sparitic texture, developed around a conduit frequently preserved at their core or filled with sulphur-bearing minerals (Figure 7(d,f)), which is suggestive of fluid venting. Oblate concretions have size in the range of several cm to a few tens, whereas the long-axis of elongated ones can be up to a few metres-long and be either laying within the bedding plane or cutting the stratigraphy. Micrite beds are parallel to bedding of the encasing sediments, have lateral continuity of a few metres, and most occur nearby elongated concretions. Internally, micrite beds can display faint parallel laminations suggesting they represent a clastic deposit rather than a concretionary product. Concretions also appear to be spatially associated with anomalous concentration tubeworm carbonates (Vestimentiferan worms) in the turbidites above, which form columnar clusters of chemoherms (Figure 7(a–c)) up to several tens of cm across and a few metres long that stand out as pinnacles due to modern erosion.

Interpretation: carbonate concretions similar to those described above has been reported from a number of depositional settings in association with biogenic methane seeps at the seafloor (Aiello et al., 2001; Campbell, 2006; 2010) and interpreted as Methane Derived Authigenic Carbonates (MDAC) precipitated thanks to anaerobic oxidation of methane sulphate reduction by microbial activity (Reitner et al., 2005). Therefore, these concretions can be interpreted as the sedimentary product of methane chimneys, whereas micrite beds may represent accumulations on the seafloor of carbonate crystals conveyed through chimneys by methane seepage. The columnar clusters of trace fossils found in the turbidites above chimney-bearing hemipelagic marlstones and levee deposits likely represent the product of focused activity of tubeworm (Vestimentiferan worms; Natalicchio et al., 2013) feeding on microbiotas associated with methane venting.

5. Discussion and conclusion

The nine channelized turbidite units mapped in this work (Annex 1) have thicknesses in the range 5–20 m, extend laterally across the whole study area, and are separated by package of hemipelagic marlstones of comparable thickness, forming a ca. 600 m-thick sedimentary succession deposited in approximately 0.5 Myr (from 7.7–7.2 Ma; Krijgsman & Langereis, 2000). Sedimentary facies character, common interleaving of amalgamated sandstone and very thin-bedded heterolithics, and orientation of channel-forms and laterally accreted bed packages altogether suggest the mapped turbidite units represent channel-levée complexes, each constituting the product of a weakly confined to unconfined network of sinuous

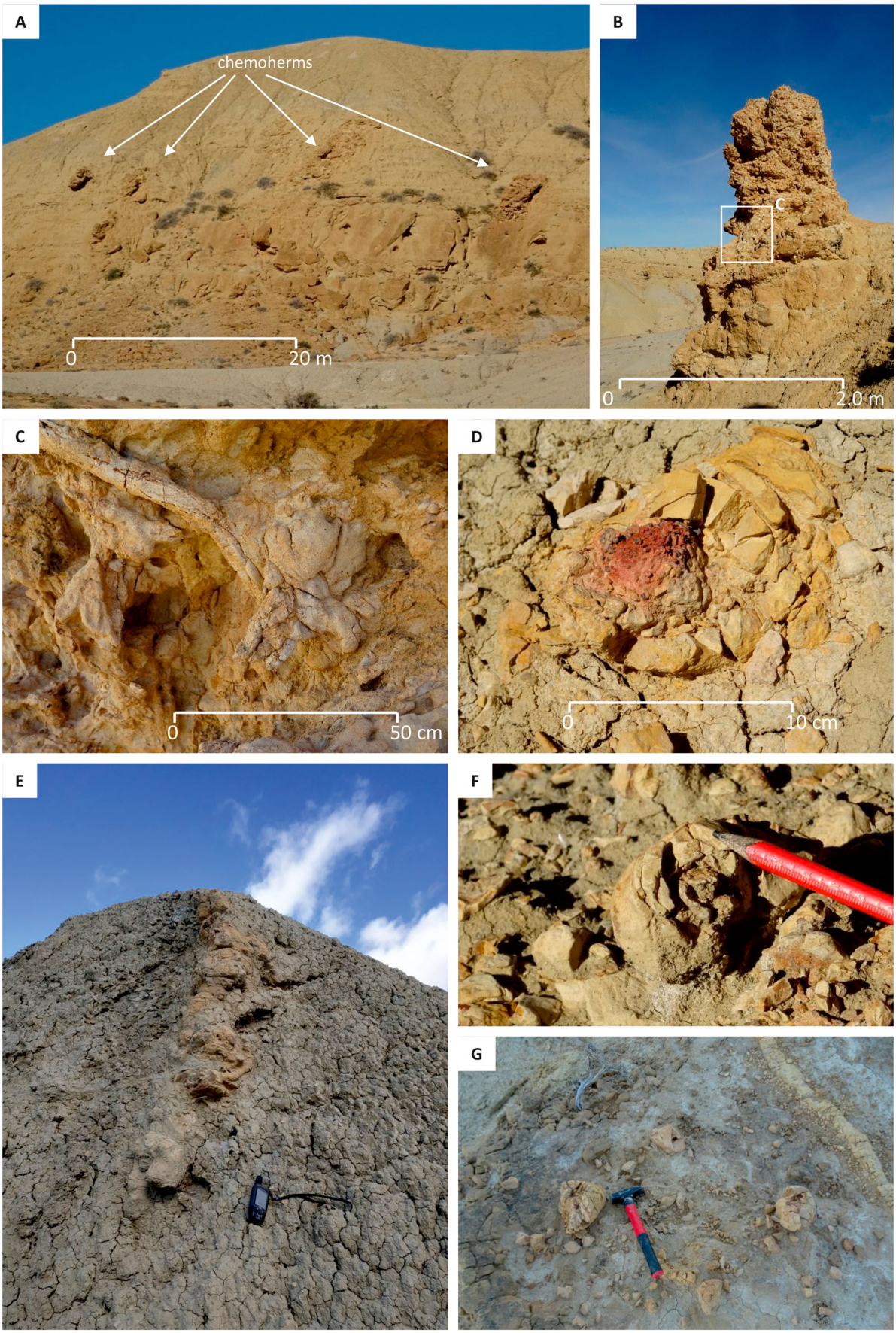

Figure 7. Carbonate concretions in many cases associated with tubeworm (chemoherms) carbonates (a) (b) (c) and conduits (d), (f) frequently occur in the presence of heterolithic levée-overbank deposits and background hemipelagic

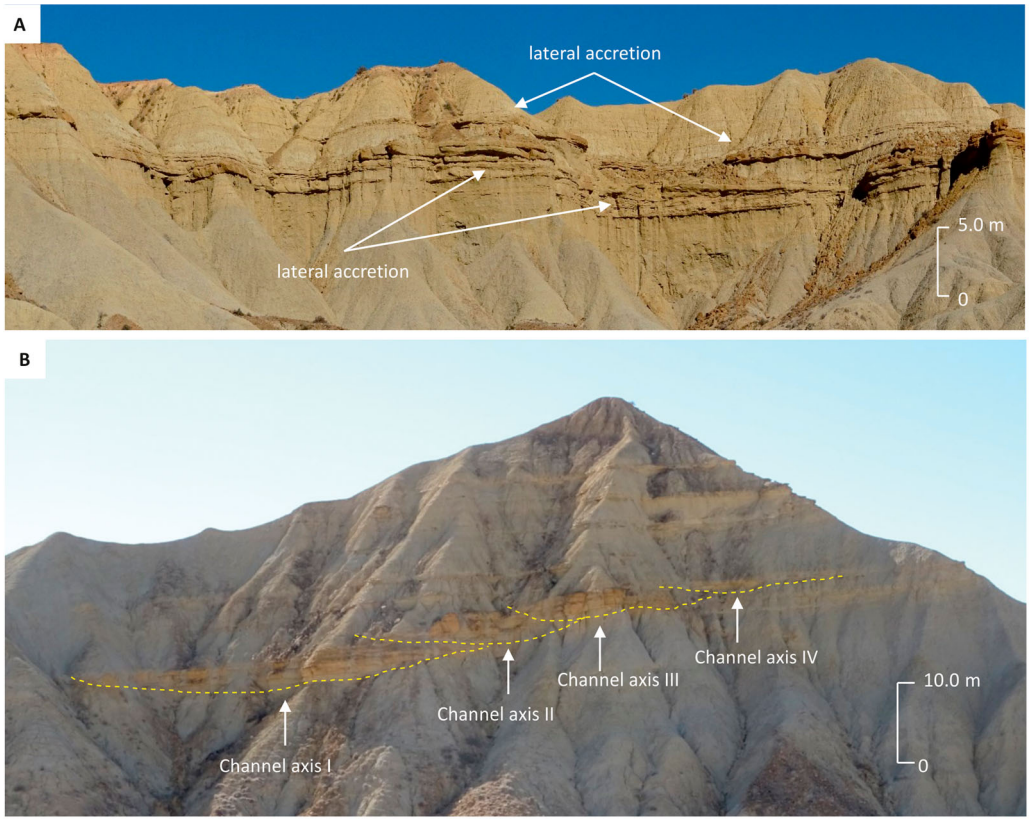

Figure 8. (a) Lateral-migration pattern. Strike section view of the Channel-levee complex 4 showing lateral accretion packages. Note how the lateral continuity of amalgamated beds sets resulting from lateral migration of channels at inner bend suggests low aggradation. (c) Vertically stacked pattern. Levéed channel (Channel-levee complex 2) belts formed by aggradational sinuous conduits.

to meandering levéed channel-belts developed across a north-dipping slope. This is in agreement with previous studies which suggested feeding of turbidity currents from the south (Gelati et al., 2000) and a sediment provenance from the Middle Atlas (Pratt et al., 2016).

The results of the mapping exercise presented in this contribution document a variety of depositional architecture styles at the scale of channel complexes. The monoclinal structure of the study area allows clearly seeing this variability on the geological map of Annex 1 from lateral continuity and proportion of sand-prone channel fills vs. mud-prone levees and hemipelagites.

Except for complexes 1, whose small channel-forms with poorly developed levèes suggest a tributary network of ephemeral channels developed on the upper slope, from older to younger, the remainder channel-levée complexes appear to become relatively sandier, with channel-fills that are increasingly more continuous laterally and amalgamated.

Field observations suggests this stratigraphic change may reflect a major turnaround of dominant type of channel belt planform (low vs. high sinuosity) and behaviour (aggradational vs. laterally shifting; Figure 8) which resulted in two-end member patterns of channel-fill stacking, namely: (a) *lateral-migration pattern* (Figure 8(a)) formed by high-sinuosity levéed channel belts which shifted laterally with minor vertical aggradational, as opposed to (b) *vertically stacked pattern* (Figure 8(b)) reflecting the vertical aggradation of low-sinuosity levéed channel belts.

The *lateral-migration pattern* is represented by subsequent amalgamated channel-fills internally showing complex cross-cutting patterns (Figure 8(a)) as a result of erosion of former deposits along the outer (or cut) bank following expansion and/or downstream sweep of meanders or beds cut-offs. The salient characteristic of this pattern is the presence of lateral accretion packages (Figure 4(a–d) and Figure 8(a)), scroll-bar-like features formed on the inner bank of channel bends as the meander expanded by eroding the cut bank. Since submarine meandering occurs when no significant aggradation takes place, the resultant sand-prone channel-fills are a composite multi-storey with rather flat geometry and of greater lateral continuity than those formed in the vertically stacked pattern (see below). The lateral migration pattern typically characterizes the complex 4, where the interweaving of sediment deposition and erosion within meandering channel-belts suggests a low sediment accommodation regime. Similar depositional architectures have been documented from a number of subsurface examples (Kolla et al., 2007; 2007; Mayall et al., 2006) and outcrop analogues (Abreu et al., 2003; 2004; Campion et al., 2012; Cronin et al., 2000;

2007; Elliott, 2000; Gamberi et al., 2013; Janocko et al., 2013; Wynn et al., 2007).

The *vertically stacked pattern* consists of subsequent channel-levée storeys with a relatively high angle of climb in strike section, which reflect a high net sediment accumulation (Figure 8(b)) typically resulting in well-developed levees preserved from later erosion. Although lateral accretion packages may be present, these are subordinate since the channels are predominantly filled in an aggradational manner. Such a pattern typically characterize complexes 2 and 3 and is comparable to those reported from a number of analogues, including the Permian Brushy Canyon Formation (Zelt & Rossen, 1995), Silurian Peary Land Group of Greenland (Surlyk, 1995), the Jurassic Stony Creek Formation of California (Campion et al., 2012), the Upper Cretaceous Juniper Ridge Conglomerate of the Great Valley Group by (Hickson & Lowe, 2002) and the Eocene–Oligocene Kirkgeçit Formation of Eastern Turkey (Cronin et al., 2000).

Although these two contrasting styles of channel-levée sedimentary architecture need to be confirmed through in-depth sedimentological investigations, the observed stratigraphic turnaround may reflect the fact that, from older to younger complex, the mapped outcrop exposes different parts of along-dip profile of the Tachrift channel belts, each showing a different balance between sediment input and accommodation regime.

Software

The geolgical map of the Tachrift channel-levee turbidite complexes was made using Esri ArcGIS 10.2 and the world imagery base map provided therein, employing the WGS84 Web Mercator (Auxiliary Shpere) projection. Map insets were made using Adobe Illustrator CS6 (study area and location maps) and GeoRose (stereo plot and rose diagram).

Acknowledgments

The authors wish to thank Andrea Baucon for the determination of bioturbations. The local Authorities of Douar Tachrift and Ras El Ksar are warmly thanked for their support during the field works.

Disclosure statement

No potential conflict of interest was reported by the author(s).

References

Abreu, V., Sullivan, M., Pirmez, C., & Mohrig, D. (2003). Lateral accretion packages (LAPs): An important reservoir element in deep water sinuous channels. *Marine and Petroleum Geology*, *20*(6-8), 631–648. https://doi.org/10.1016/j.marpetgeo.2003.08.003

Aiello, I. W., Garrison, R. E., Moore, J. C., Kastner, M., & Stakes, D. S. (2001). Anatomy and origin of carbonate structures in a Miocene cold-seep field. *Geology*, *29*(12), 1111–1114. https://doi.org/10.1130/0091-7613(2001)029<1111:AAOOCS>2.0.CO;2

Armitage, D. A., Romans, B. W., Covault, J. A., & Graham, S. A. (2009). The influence of mass-transport-deposit surface topography on the evolution of turbidite architecture: The Sierra Contreras, Tres Pasos Formation (Cretaceous), southern Chile. *Journal of Sedimentary Research*, *79*(5), 287–301. https://doi.org/10.2110/jsr.2009.035

Beaubouef, R. T. (2004). Deep-water leveed-channel complexes of the Cerro Toro Formation, upper Cretaceous, southern Chile. *American Association of Petroleum Geology Bulletin*, *88*, 1471–1500. https://doi.org/10.1306/06210403130

Bernini, M., Boccaletti, M., Gelati, R., Moratti, G., Papani, G., & Mokhtari, J. E. (1999). Tectonics and sedimentation in the Taza-Guercif basin, northern Morocco: Implications for the Neogene evolution of the Rif-Middle Atlas orogenic system. *Journal of Petroleum Geology*, *22*(1), 115–128. https://doi.org/10.1111/j.1747-5457.1999.tb00462.x

Bernini, M., Boccaletti, M., Moratti, G., & Papani, G. (2000). Structural development of the Taza-Guercif basin as a constraint for the Middle Atlas shear Zone tectonic evolution. *Marine and Petroleum Geology*, *17*(3), 391–408. https://doi.org/10.1016/S0264-8172(99)00042-2

Boccaletti, M., Gelati, R., Papani, G., Bernini, M., El Mokhtari, J., & Moratti, G. (1990). The Gibraltar Arc: An example of neoalpine arcuate deformation connected with ensialic shear zones. Memorie della Societa Geologica Italiana, *45*, 409–423.

Camacho, H., Busby, C. J., & Kneller, B. (2002). A new depositional model for the classical turbidite locality at San Clemente State Beach, California. *American Association of Petroleum Geologist*, *86*, 1543–1560. https://doi.org/10.1306/61EEDCF6-173E-11D7-8645000102C1865D

Campbell, K. A. (2006). Hydrocarbon seep and hydrothermal vent paleoenvironments and paleontology: Past developments and future research directions. *Palaeogeography, Palaeoclimatology, Palaeoecology*, *232* (2-4), 362–407. https://doi.org/10.1016/j.palaeo.2005.06.018

Campion, K. M., Sprague, A. R., Mohrig, D., Lovell, R. W., Drzewiecki, P. A., Sullivan, M. D., Ardill, J. A., Jensen, G. N., & Sickafoose, D. K. (2003). *Outcrop expression of confined channel complexes*.

Campion, K. M., Sprague, A. R., Mohrig, D., Lovell, R. W., Drzewiecki, P. A., Sullivan, M. D., Ardill, J. A., Jensen, G. N., & Sickafoose, D. K. (2012). Outcrop expression of confined channel complexes. In: *Deep-water reservoirs of the world*: 20th Annual, 127–150.

Chalouan, A., Michard, A., El Kadiri, K., Negro, F., de Lamotte, D. F., Soto, J. I., & Saddiqi, O. (2008). The Rif belt. In *Continental evolution: The geology of Morocco* (pp. 203–302). Springer.

Cronin, B. T. (1995). Structurally-controlled deep sea channel courses: Examples from the Miocene of southeast Spain and the Alboran Sea, southwest Mediterranean. *Geological Society, London, Special Publications*, *94*(1), 115–135. https://doi.org/10.1144/GSL.SP.1995.094.01.10

Cronin, B. T., Hurst, A., Celik, H., & Türkmen, I. (2000). Superb exposure of a channel, levee and overbank complex in an ancient deep-water slope environment.

Sedimentary Geology, *132*(3-4), 205–216. https://doi.org/10.1016/S0037-0738(00)00008-7

de Lamotte, D. F., Leturmy, P., Missenard, Y., Khomsi, S., Ruiz, G., Saddiqi, O., Guillocheau, F., & Michard, A. (2009). Mesozoic and Cenozoic vertical movements in the Atlas system (Algeria, Morocco, Tunisia): an overview. *Tectonophysics*, *475*(1), 9–28. https://doi.org/10.1016/j.tecto.2008.10.024

Dela Pierre, F., Martire, L., Natalicchio, M., Clari, P., & Petrea, C. (2010). Authigenic carbonates in upper Miocene sediments of the Tertiary Piedmont basin (NW Italy): Vestiges of an ancient gas hydrate stability zone? *GSA Bulletin*, *122*, 994–1010. https://doi.org/10.1130/B30026.1

Di Celma, C. N., Brunt, R. L., Hodgson, D. M., Flint, S. S., & Kavanagh, J. P. (2011). Spatial and Temporal Evolution of a Permian submarine slope channel-levee system, Karoo basin, South Africa. *Journal of Sedimentary Research*, *81*(8), 579–599. https://doi.org/10.2110/jsr.2011.49

Dykstra, M., & Kneller, B. (2007). Canyon San Fernando, Mexico: A deep-water, channel-levee complex exhibiting evolution from submarine canyon-confined to unconfined. Atlas deep. Outcrops AAPG. *Studies of Geology*, *56*, 226–230. DOI: 10.1306/1240943St563284

El Kati, I., Benammi, M., Tabhaoui, H., & Benammi, M. (2017). Magnetostratigraphy of Neogene series of Guercif basin (Morocco). *Rev la Societa Geológica Españaa*, *30*, 37–50.

Elliott, T. & Others (2000). Depositional architecture of a sand-rich, channelized turbidite system: The upper Carboniferous Ross sandstone Formation, western Ireland. *Deep Reserve World*, 342–373.

Eschard, R., Albouy, E., Deschamps, R., Euzen, T., & Ayub, A. (2003). Downstream evolution of turbiditic channel complexes in the Pab range outcrops (Maastrichtian, Pakistan). *Marine and Petroleum Geology*, *20*(6-8), 691–710. https://doi.org/10.1016/j.marpetgeo.2003.02.004

Felletti, F. (2016). Depositional architecture of a confined, sand-rich submarine system: The Bric la Croce-Castelnuovo turbidite system (Tertiary Piedmont basin, Oligocene, NW Italy). *Italian Journal of Geosciences*, *135*(3), 365–382. https://doi.org/10.3301/IJG.2015.15

Figueiredo, J. J. P., Hodgson, D. M., Flint, S. S., & Kavanagh, J. P. (2013). Architecture of a channel complex formed and filled during long-term degradation and entrenchment on the upper submarine slope, unit F, Fort Brown Fm., SW Karoo basin, South Africa. *Marine and Petroleum Geology*, *41*, 104–116. https://doi.org/10.1016/j.marpetgeo.2012.02.006

Fonnesu, F. (2003). 3D seismic images of a low-sinuosity slope channel and related depositional lobe (West Africa deep-offshore). *Marine and Petroleum Geology*, *20*(6-8), 615–629. https://doi.org/10.1016/j.marpetgeo.2003.03.006

Fonnesu, M., & Felletti, F. (2019). Facies and architecture of a sand-rich turbidite system in an evolving collisional-trench basin: A case history from the upper Cretaceous-Palaeocene Gottero system (NW Apennines). *Rivista Italiana. di Paleontol. e Stratigr*, *125*, 449–487. https://doi.org/10.13130/2039-4942/11789

Gamberi, F., Rovere, M., Dykstra, M., Kane, I. A., & Kneller, B. C. (2013). Integrating modern seafloor and outcrop data in the analysis of slope channel architecture and fill. *Marine and Petroleum Geology*, *41*, 83–103. https://doi.org/10.1016/j.marpetgeo.2012.04.002

Gardner, M. H., Borer, J. M., Melick, J. J., Mavilla, N., Dechesne, M., & Wagerle, R. N. (2003). Stratigraphic process-response model for submarine channels and related features from studies of Permian Brushy Canyon outcrops, West Texas. *Marine and Petroleum Geology*, *20*(6-8), 757–787. https://doi.org/10.1016/j.marpetgeo.2003.07.004

Gelati, R., Moratti, G., & Papani, G. (2000). The late Cenozoic sedimentary succession of the Taza-Guercif basin, south Rifian Corridor, Morocco. *Marine and Petroleum Geology*, *17*(3), 373–390. https://doi.org/10.1016/S0264-8172(99)00054-9

Gomez, F., Barazangi, M., & Demnati, A. (2000). Structure and evolution of the Neogene Guercif basin at the junction of the Middle Atlas mountains and the Rif thrust belt, Morocco. *Am. Assoc. Pet. Geol. Bull*, *84*, 1340–1364. https://doi.org/10.1306/A9673EA0-1738-11D7-8645000102C1865D

Hansen, L. A. S., Callow, R. H. T., Kane, I. A., Gamberi, F., Rovere, M., Cronin, B. T., & Kneller, B. C. (2015). Genesis and character of thin-bedded turbidites associated with submarine channels. *Marine and Petroleum Geology*, *67*, 852–879. https://doi.org/10.1016/j.marpetgeo.2015.06.007

Hickson, T. A., & Lowe, D. R. (2002). Facies architecture of a submarine fan channel–levee complex: The Juniper Ridge Conglomerate, Coalinga, California. *Sedimentology*, *49*(2), 335–362. https://doi.org/10.1046/j.1365-3091.2002.00447.x

Hubbard, S. M., Covault, J. A., Fildani, A., & Romans, B. W. (2014). Sediment transfer and deposition in slope channels: Deciphering the record of enigmatic deep-sea processes from outcrop. *Geological Society of America Bulletin*, *126*(5-6), 857–871. https://doi.org/10.1130/B30996.1

Janocko, M., Nemec, W., Henriksen, S., & Warchoł, M. (2013). The diversity of deep-water sinuous channel belts and slope valley-fill complexes. *Marine and Petroleum Geology*, *41*, 7–34. https://doi.org/10.1016/j.marpetgeo.2012.06.012

Kane, I. A., & Hodgson, D. M. (2011). Sedimentological criteria to differentiate submarine channel levee subenvironments: Exhumed examples from the Rosario Fm. (upper Cretaceous) of Baja California, Mexico, and the Fort Brown Fm. (Permian), Karoo basin. *Marine and Petroleum Geology*, *28*(3), 807–823. https://doi.org/10.1016/j.marpetgeo.2010.05.009

Kane, I. A., Kneller, B. C., Dykstra, M., Kassem, A., & McCaffrey, W. D. (2007). Anatomy of a submarine channel-levee: An example from upper Cretaceous slope sediments, Rosario Formation, Baja California, Mexico. *Marine and Petroleum Geology*, *24*(6-9), 540–563. https://doi.org/10.1016/j.marpetgeo.2007.01.003

Kneller, B., Bozetti, G., Callow, R., Dykstra, M., Hansen, L., Kane, I., Li, P., McArthur, A., Catharina, A. S., Dos Santos, T. & Others (2020). Architecture, process, and environmental diversity in a late Cretaceous slope channel system. *Journal of Sedimentary Research*, *90*(1), 1–26. https://doi.org/10.2110/jsr.2020.1

Kolla, V., Posamentier, H. W., & Wood, L. J. (2007). Deep-water and fluvial sinuous channels characteristics, similarities and dissimilarities, and modes of formation. *Marine and Petroleum Geology*, *24*(6-9), 388–405. https://doi.org/10.1016/j.marpetgeo.2007.01.007

Krijgsman, W., & Langereis, C. G. (2000). Magnetostratigraphy of the Zobzit and Koudiat Zarga sections (Taza-Guercif basin, Morocco): Implications for the evolution of the Rifian Corridor. *Marine and Petroleum Geology*, *17*(3), 359–371. https://doi.org/10.1016/S0264-8172(99)00029-X

Krijgsman, W., Langereis, C. G., Zachariasse, W. J., Boccaletti, M., Moratti, G., Gelati, R., Iaccarino, S., Papani, G., & Villa, G. (1999). Late Neogene evolution of the Taza–guercif basin (Rifian Corridor, Morocco) and implications for the Messinian salinity crisis. *Marine Geology*, *153*(1-4), 147–160. https://doi.org/10.1016/S0025-3227(98)00084-X

Labourdette, R. (2007). Integrated three-dimensional modeling approach of stacked turbidite channels. *American Association of Petroleum Geology Bulletin*, *91*, 1603–1618. https://doi.org/10.1306/06210706143

Li, P., Kneller, B., Thompson, P., Bozetti, G., & dos Santos, T. (2018). Architectural and facies organisation of slope channel fills: Upper Cretaceous Rosario Formation, Baja California, Mexico. *Marine and Petroleum Geology*, *92*, 632–649. https://doi.org/10.1016/j.marpetgeo.2017.11.026

Macauley, R. V., & Hubbard, S. M. (2013). Slope channel sedimentary processes and stratigraphic stacking, Cretaceous Tres Pasos Formation slope system, Chilean Patagonia. *Marine and Petroleum Geology*, *41*, 146–162. https://doi.org/10.1016/j.marpetgeo.2012.02.004

Mayall, M., Jones, E., & Casey, M. (2006). Turbidite channel reservoirs-Key elements in facies prediction and effective development. *Marine and Petroleum Geology*, *23*(8), 821–841. https://doi.org/10.1016/j.marpetgeo.2006.08.001

Mayall, M., & Stewart, I. (2012). The architecture of turbidite slope channels. In: *deep-water reservoirs of the world: 20th Annual*, 578–586.

McHargue, T., Pyrcz, M. J., Sullivan, M. D., Clark, J. D., Fildani, A., Romans, B. W., Covault, J. A., Levy, M., Posamentier, H. W., & Drinkwater, N. J. (2011). Architecture of turbidite channel systems on the continental slope: Patterns and predictions. *Marine and Petroleum Geology*, *28*(3), 728–743. https://doi.org/10.1016/j.marpetgeo.2010.07.008

Natalicchio, M., Pierre, F. D., Clari, P., Birgel, D., Cavagna, S., Martire, L., & Peckmann, J. (2013). Hydrocarbon seepage during the Messinian salinity crisis in the Tertiary Piedmont basin (NW Italy). *Palaeogeography, Palaeoclimatology, Palaeoecology*, *390*, 68–80. https://doi.org/10.1016/j.palaeo.2012.11.015

Piper, D. J. W., Hiscott, R. N., & Normark, W. R. (1999). Outcrop-scale acoustic facies analysis and latest Quaternary development of Hueneme and Dume submarine fans, offshore California. *Sedimentology*, *46*(1), 47–78. https://doi.org/10.1046/j.1365-3091.1999.00203.x

Posamentier, H. W., & Kolla, V. (2003). Seismic geomorphology and stratigraphy of depositional elements in deep-water settings. *Journal of Sedimentary Research*, *73*(3), 367–388. https://doi.org/10.1306/111302730367

Pratt, J. R., Barbeau, D. L., Izykowski, T. M., Garver, J. I., & Emran, A. (2016). Sedimentary provenance of the Taza-Guercif basin, south Rifean Corridor, Morocco: Implications for basin emergence. *Geosphere*, *12*(1), 221–236. https://doi.org/10.1130/GES01192.1

Pyles, D. R., Jennette, D. C., Tomasso, M., Beaubouef, R. T., & Rossen, C. (2010). Concepts learned from a 3D outcrop of a sinuous slope channel complex: Beacon channel complex, Brushy Canyon Formation, West Texas, U.S.A. *Journal of Sedimentary Research*, *80*(1), 67–96. https://doi.org/10.2110/jsr.2010.009

Reitner, J., Peckmann, J., Reimer, A., Schumann, G., & Thiel, V. (2005). Methane-derived carbonate build-ups and associated microbial communities at cold seeps on the lower Crimean shelf (Black Sea). *Facies*, *51*(1-4), 66–79. https://doi.org/10.1007/s10347-005-0059-4

Samuel, A., Kneller, B., Raslan, S., Sharp, A., & Parsons, C. (2003). Prolific deep-marine slope channels of the Nile Delta, Egypt. *American Association of Petroleum Geology Bulletin*, *87*, 541–560. https://doi.org/10.1306/1105021094

Sani, F., Zizi, M., & Bally, A. W. (2000). The Neogene-Quaternary evolution of the Guercif basin (Morocco) reconstructed from seismic line interpretation. *Marine and Petroleum Geology*, *17*(3), 343–357. https://doi.org/10.1016/S0264-8172(99)00058-6

Sullivan, M., Jensen, G., Goulding, F., Jennette, D., Foreman, L., & Stern, D. (2000). Architectural analysis of deep-water outcrops: Implications for exploration and development of the Diana sub-basin, western Gulf of Mexico. In: *Deep-water reservoirs of the world: Gulf Coast Section SEPM Foundation 20th Annual Research Conference*, 1010–1032.

Surlyk, F. (1995). Deep-sea fan valleys, channels, lobes and fringes of the Silurian Peary Land Group, north Greenland. In *Atlas of deep water Environments* (pp. 124–138). Springer.

Sylvester, Z., Pirmez, C., & Cantelli, A. (2011). A model of submarine channel-levee evolution based on channel trajectories: Implications for stratigraphic architecture. *Marine and Petroleum Geology*, *28*(3), 716–727. https://doi.org/10.1016/j.marpetgeo.2010.05.012

Walker, R. G. (1975). Nested submarine-fan channels in the capistrano formation, San Clemente, California. *Geological Society of America Bulletin*, *86*(7), 915–924. https://doi.org/10.1130/0016-7606(1975)86<915:NSCITC>2.0.CO;2

Weimer, P., Slatt, R. M., Coleman, J., Rosen, N. C., Nelson, H., Bouma, A. H., Styzen, M. J., & Lawrence, D. T. (2000). *Deep-water reservoirs of the world.*

Wynn, R. B., Cronin, B. T., & Peakall, J. (2007). Sinuous deep-water channels: Genesis, geometry and architecture. *Marine and Petroleum Geology*, *24*(6-9), 341–387. https://doi.org/10.1016/j.marpetgeo.2007.06.001

Zelt, F., & Rossen, C. (1995). *An atlas of deep-water environments: Architectural style in turbidite systems.*

Annex 1. Geologica map of the Tachrift channel-levée turbidite complexes (Tortonian) of the Taza-Guercif Basin (South Rifian Corridor, NE Morocco).